

RUBBER PARTICLE SIZE EFFECT ON IMPACT CHARACTERISTICS OF PC/ABS (50/50) BLENDS

M. Nizar Machmud, Masaki Omiya, Hirotsugu Inoue and Kikuo Kishimoto
Department of Mechanical and Control Engineering
Tokyo Institute of Technology
O-okayama 2-12-1, Meguro-ku, Tokyo, 152-8550

ABSTRACT

This paper presents an investigation of effect of rubber particle size distributed in acrylonitrile-butadiene-styrene (ABS) system on impact failure characteristics of two grades of polycarbonate (PC)/ABS (50/50) blends. This work was carried out by use of an instrumented-drop weight impact test performed at room temperature under a range of loading rates. Effect of the rubber particle size on the failure characteristics of PC/ABS (50/50) blends has been investigated on the blends containing rubber of about 10 wt%. The failure modes of the tested materials induced by a hemispherical tip-ended striker were quite similar at the loading rates of 2 and 4 m/sec but they were different at 3 m/sec. Both of the grades were found to break in brittle manner beyond 3 m/sec. In case of the blends with rubber particle size of 270 nm, all of the blends were found in shattering when loading rate exceeds 2 m/sec. In a case of rubber particle size of 150-170 nm, however, the blends were found to break in semi ductile manner with a couple of stress whitening regions localized over each crack tip at 3 m/sec. These test results reveal that at the rubber content, variation of the smaller rubber particle sizes distributed in ABS not only improves the ductility of the blends but it also has a significant contribution in the increasing impact energy of the blends. Two grades of ABS materials containing rubber of about 10% were then tested to further study the influence of the ABS type blended into the polycarbonate material. At similar condition, these test series also reveal that blending brittle ABS into the polycarbonate produces tough PC/ABS blend. Furthermore, analyzing using scanning electron microscope (SEM) on fracture surface of the specimen of each blend correlates well the testing results.

Introduction

Blending and addition of rubber particles have been the common concepts to improve the strength and fracture toughness of polymeric materials. Polycarbonate (PC) has been well known as a tough polymer. In some particular conditions, polycarbonate loses its tough character and exhibits brittle fracture [1-3]. Blending acrylonitrile-butadiene-styrene (ABS) into the polycarbonate not only reduces its sensitivity to the conditions but also leads to creating materials with new characteristics. This blend has been known as a ternary blend, because ABS itself usually consists of polybutadiene (PB) rubber embedded within a matrix of styrene-acrylonitrile copolymer (SAN). This blend has become a frequently used engineering material due to combining several advantageous properties of both components.

PC/ABS blends have been the subject of many studies and their behaviors have also been reported in a numerous published scientific works. They have revealed that properties of such ternary blend strongly depend on the structure properties of the components and morphology of the blends depends on blending and injection moulding conditions [2]. At an ABS volume fraction of about 50%, microstructure of the blend shows a co-continuous morphology [4]. Extensive studies on this type have rarely found, most of the published research works have mainly focused on dispersed types of the blends while recently many industrial products made of the blends are the co-continuous types. Yet, the works have been carried out using notched specimens that measure only propagation energy, not crack initiation energy, and thus, they do not give a 'true' indicating impact resistance of the materials. Selection of the material and proposing a practical test are thus the reason of this present work to gain insight into the behavior of the co-continuous blends.

Fracture experiments performed on the co-continuous PC/ABS blends indicated contents of rubber embedded within SAN were about 10-15 wt%. At 15 wt% PB in SAN, delamination due to failure of the PC/ABS interface was observed and it was not found when rubber content in ABS was increased [4-6]. Toughness of blends was enhanced and their strength was improved as well with increasing the content of rubber in ABS. Effect of the rubber particle size distributed in the co-continuous blends, however, has not been yet reported. The aim of this work, therefore, is to study the effect of rubber particle size distributed in ABS on the impact failure characteristics of the co-continuous PC/ABS blends. Because fracture behavior of a material is

complex and strongly depends on a type of test [7], this study is carried out by use of a drop weight impact testing apparatus in order to correlate the test results of the materials to a particular practical impact condition. Since impact loading rate has often been used as an indicator in failure characteristics classification of a target, the goal of this study is to analyze the response of two grades of PC/ABS (50/50) blends containing rubber of about 10% affected by rubber particle size and to describe definite alteration of the blends under a range of loading rates.

Materials

The PC/ABS (50/50) blends used in this study are PC/ABS (50/50) blends containing rubber of about 10 wt% which are classified according to distribution of rubber particle size in ABS to be monomodal (270 nm) and bimodal (150-170 nm) types. Influence of the ABS on impact characteristics of the blends is also studied by testing the ABS constituent of each blend: ABS materials containing rubber of about 10 wt% blended into a PC material with molecular weight of about 22500 g/mol. In all, four grades of structural plastics are tested. They are two grades of ABS and two grades of PC/ABS (50/50) blends as shown in Table 1.

Table 1. ABS and PC/ABS (50/50) blends materials used for testing

	ABS-1 (10 wt% rubber) Ø 270 nm	ABS-2 (10 wt% rubber) Ø150-170 nm
PC (22500 g/mol)	PA-1 (50%:50%)	PA-2 (50%:50%)

Mechanical Testing: Drop Weight Impact Test

The drop weight impact testing apparatus is outfitted with instruments to measure a digital impact force-time history during impact at room temperature. The impact force-time data is then converted to obtain impact force-striker displacement behavior of the materials. Impact energy is a measure of material toughness defined as the area under impact force-displacement. Behavior of the blends induced by a hemispherical tip ended-cylindrical impactor made of stainless steel (SS55) with diameter of 20 mm. The impactor strikes perpendicularly the center of the simply-supported circular thin plate. The specimens have a diameter of 99.3 mm and initial thickness of 2 mm. The testing set-up is schematically illustrated in Figure 1. The body of the impactor attached to guiding rods is designed to give a total impactor mass of 2.4 kg. The specimens are tested at impact loading rates of about 2 m/s (6.56 ft/s), 3 m/s (9.84 ft/s) and 4 m/s (13 ft/s). The range of impact loading rates v is defined as given in Eq. 1.

$$v = \sqrt{2gh_d} \tag{1}$$

where g is the acceleration due to gravity, and h_d is drop height measured during the impact tests. Although the loading rate prediction was presumed to be accurate, the actual rate may be lower than the measured rate due to friction on the guiding rods. However, the effect of friction on the accuracy of loading rate prediction using the formula is negligible [8].

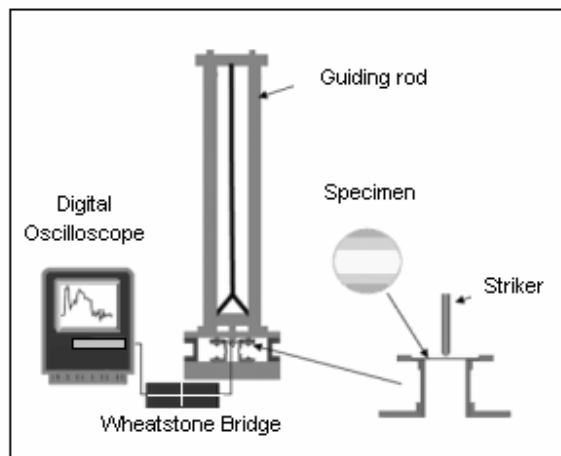


Figure 1. Illustration of the instrumented-drop weight impact test

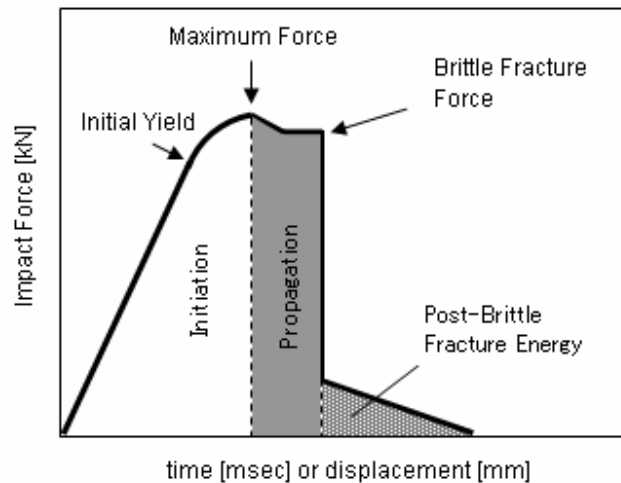


Figure 2. Schematic representation of impact force-time/displacement behavior obtained from a drop weight impact test

Not like a testing on notched specimens that measures only propagation energy, not crack initiation energy, and they thus do not give a true indicating impact resistance of the specimen, this test provides an indication of the energy for both the initiation and propagation of a crack. Figure 2 represents the impact force-time obtained from a drop weight impact test. From the representative impact force-time curve one can distinguish ductile from brittle failure and crack initiation from crack propagation energy. Crack initiation part is assumed to take place from the initial point up to the point of maximum impact force and after the point to the end is the part of crack propagation. Further, area under the first part is used for indicating the crack initiation energy and area under the latter part is used for indicating the crack propagation energy.

Microscopic Observation: SEM

As morphology of the blends plays an important role in the drop weight impact behavior, it is necessary to characterize their fracture behaviors after the impact tests. The behaviors are characterized on deformation and fracture surface of specimen. Both of the behaviors are analyzed using a scanning electron microscope (SEM, JEOL JSM-5300T). Only deformation behavior over a crack tip in PA-2 blend specimen tested under 3 m/sec is analyzed and SEM micrograph magnifications are set to 50, 1000 and 2000 at 15 kV accelerating voltage. The SEM micrographs for fracture surface of the specimen of each blend that failed at 3 m/sec are set to be magnification of 350, 500, 2000 and 5000 at 10 kV accelerating voltage. Definite alteration of deformation behavior between PA-1 and PA-2 tested under the rate of 3 m/sec is then described by capturing closer views of a radial cracking formation near the impacted point taken at an oblique angle. Since under the rate of 3 m/sec PA-1 specimen shattered, the SEM micrographs are therefore taken on the arrested tearing crack of the shattered specimen. For the latter task, SEM micrograph magnifications are set to 1000 and 2000 at 10 kV accelerating voltage.

Results and Discussion

Failure modes with presence of radial cracking formation were exhibited in both of the blends. However, the typical drop weight impact loading behavior at which the specimens exhibited a more localized response near the impacted point can only be found on tougher materials. In general, these tests revealed that all of the blends fractured in brittle modes when the rate of loading exceeded 3 m/sec. Figures 3 and 4 shows typical impact force-time histories and failure features of PA-1 and PA-2, respectively. The blends exhibited quite similar behavior under 2 and 4 m/sec. However, at 3 m/sec, their failure modes were totally different. PA-1 specimens showed very few of plastic deformation and fractured in brittle modes without crazing due to rapid running of the crack that leaving a relatively flat surface at the break while PA-2 specimens demonstrated a larger amounts of plastic deformation and fractured in semi ductile modes with damage indicated by a couple of stress whitening regions localized over each crack tip. From the failure features of the PA-2 tested 3 m/sec one can see the plastic deformation forming a pyramidal formation of the stress whitening behaviors.

ABS materials were also tested in order to investigate contribution of the ABS materials on the behavior of the blends. In general, ABS-1 materials failed in semi ductile manner and showed a wide couple of stress whitening regions localized in surrounding of the crack beyond 2 m/sec whereas all ABS-2 materials failed in brittle manner.

Indicator of resistance of the PA-1 and PA-2 blends to the crack under impact can be distinguished from Figures 5 and 6, respectively. PA-1 blend have much higher initiation energy than the propagation energy while initiation energy and

propagation energy of PA-2 blend are better than those of PA-1 blend and their portion are relatively equal under higher loading rates. In general, impact force of the blends and ABS materials increased with increasing the loading rates (see Figure 7). The PA-1 blend showed the highest impact strength and according to the slope made on the plot, impact strength of PA-1 specimens were relatively more sensitive to the applied loading rates than that of PA-2 blend. Impact energy measured from the whole area under the impact force-displacement curve is used for characterizing impact behavior of the blends and ABS materials. Impact energy of the blends and ABS materials also increased with increasing the loading rate and they then decreased under a certain loading rate at which failure occurred. However, impact energy of PA-1 specimens tended to decrease with increasing the loading rate and their values were quite lower compare to that of PA-2 specimen and ABS-1 under 3 and 4 m/sec as seen in Figure 8. Impact energy of the materials showed high sensitivity to the applied loading rates.

Comparison between ABS-1 and ABS-2 materials is plotted in impact force and impact energy as function of loading rate as shown in Figure 8. These results reveal that ABS-1 materials are tougher and the measured parameters are more sensitive to the applied loading rates than ABS-2 materials.

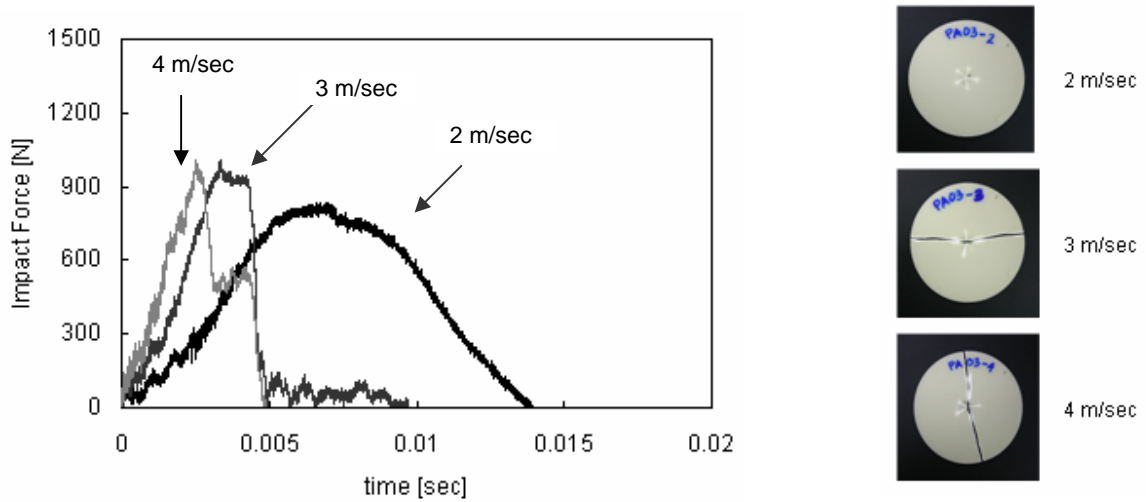


Figure 3. Impact force-time histories of PA-1 and their features under different loading rates at 296 K (room temperature)

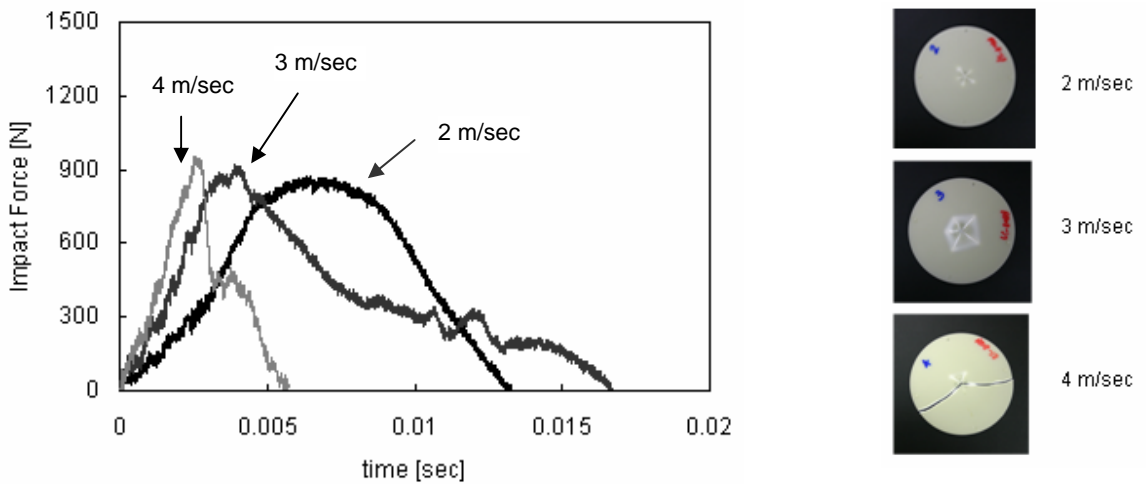


Figure 4. Impact force-time histories of PA-2 and their features under different loading rates at 296 K (room temperature)

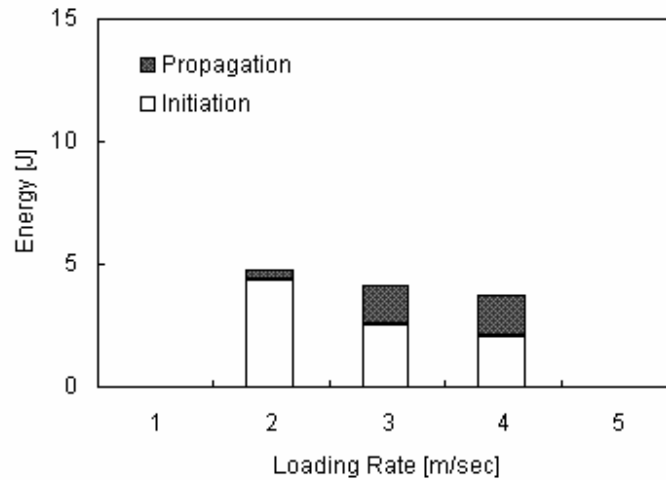


Figure 5. Impact energy distribution of PA-1 blend

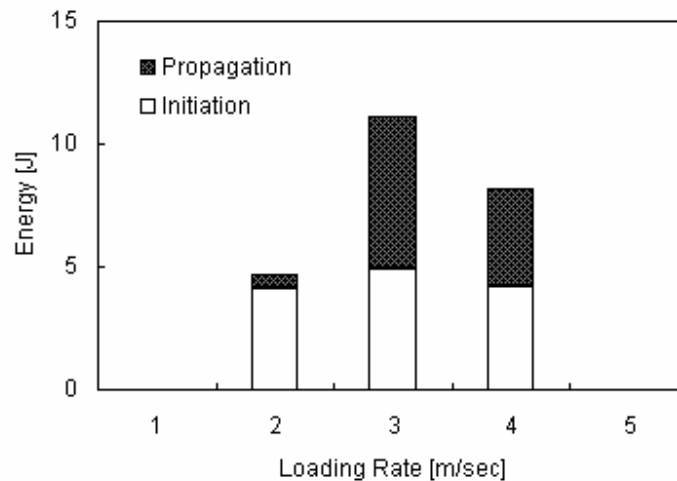


Figure 6. Impact energy distribution of PA-2 blend

SEM investigation over the crack tip shows a pattern leading the higher resistance of the PA-2 blend to the crack propagation with promoting the stress whitening (see Figure 9). Figures 10 and 11 show respectively SEM observation micrographs of PA-1 and PA-2 blends tested under 3 m/sec taken on the fracture surface of the specimen. PA-1 blend that fractured in brittle manner exhibited one mode of failure that might be contributed by shear crack and a few of tension crack. They are clearly drawn in both of the low and higher magnification micrographs as described in Figures 10. In fact, the PA-2 blend that fractured in semi-ductile manner had two modes of failure on the surrounding of its fracture surface. Low magnification micrographs of the fracture surface of the PA-2 blend (see Figures 11a and 11b) show the two modes of failure that might be highly contributed by tension, shear and tearing cracks as described clearly Figure 11c. From the higher magnification micrograph, one can see that PA-2 blend exhibited the higher resistance to crack propagation under impact rather than PA-1 blend.

SEM observation near the impacted point shows PA-1 blend displayed delamination like-formation (see Figure 12) whereas PA-2 blend showed fibril-like formation zone as seen in Figure 13. Any delamination in PA-2 blend was not found. This observation results confirm the results pointed previously by other worker [4,5].

These tests series also reveal that blending the PC with tougher ABS creates brittle PC/ABS blends. On the other hand, blending the PC with brittle ABS creates tough PC/ABS blends, i.e. size variation of smaller rubber particle distributed in ABS reduced the impact energy of the ABS but it enhanced the impact energy of PC/ABS (50/50) blends. The results also indicated that the PC/ABS (50/50) blends have significantly higher resistance to crack initiation as well as to crack propagation under

high strain rates due to the variation of the smaller rubber particle size. These test series also reveal that presence the large monomodal particle in ABS system improves the strength of the blends but in other hand it reduces their toughness.

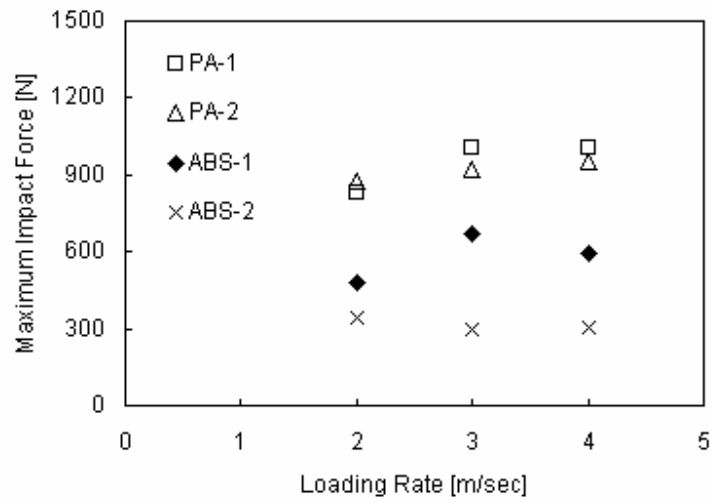


Figure 7. Maximum impact force-loading rate plot of the tested materials

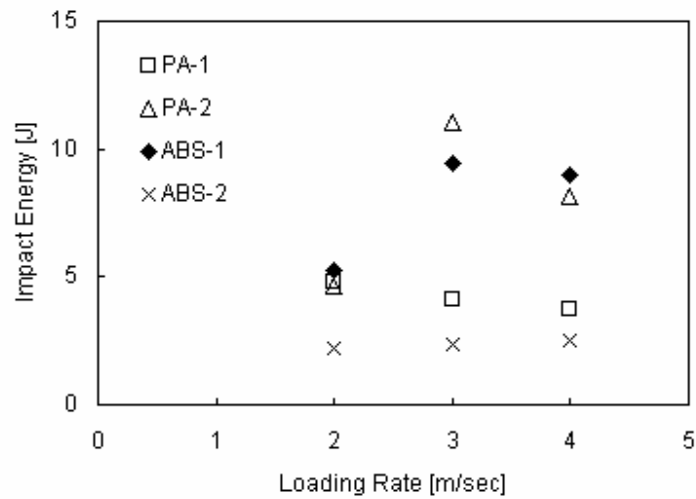


Figure 8. Impact energy-loading rate plots of the tested materials

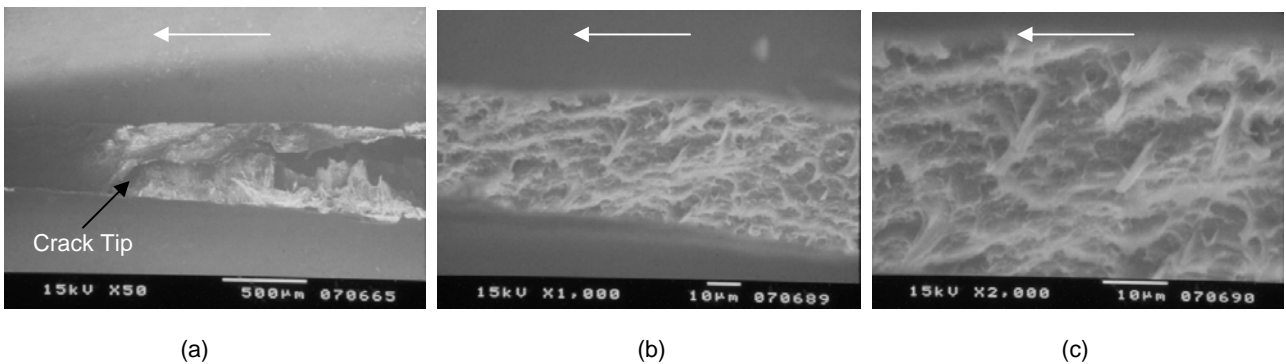


Figure 9. Top view SEM micrographs taken over crack tip of failed specimen for PA-2 blend tested under 3 m/sec. White arrows indicate the direction of fracture.

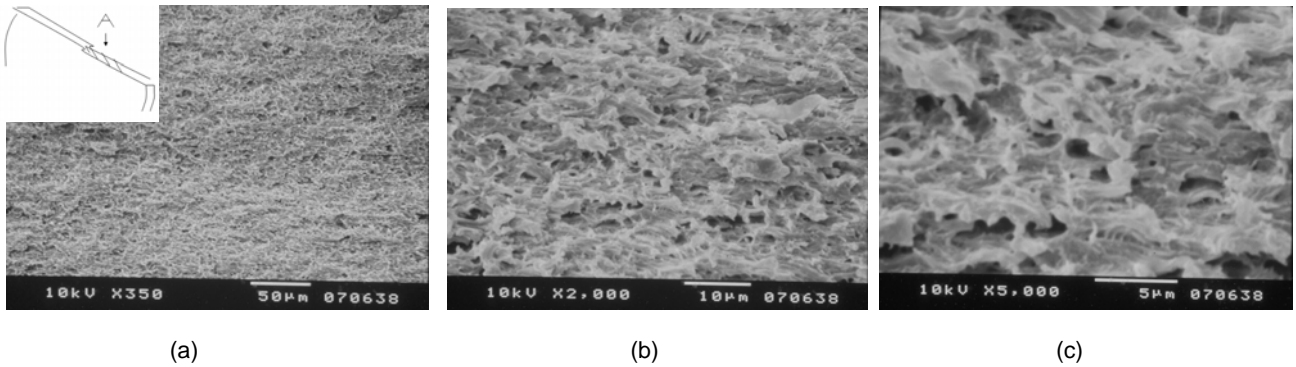


Figure 10. SEM micrographs of drop weight impact-fractured surface of PA-1 blend tested under 3 m/sec: (a) low magnification, (b) and (c) higher magnification. The inset in (a) describes the SEM observation on fracture surface (shaded).

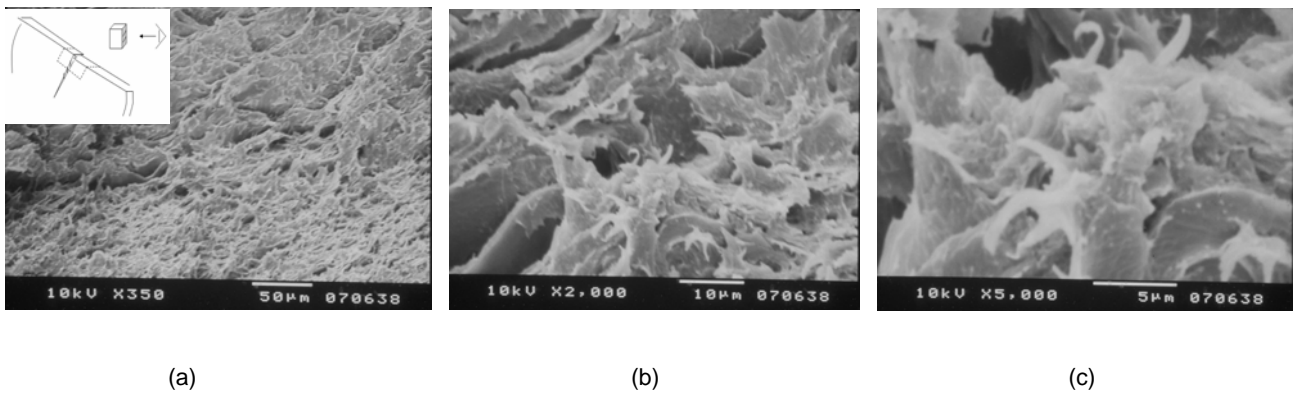


Figure 11. SEM micrographs of drop weight impact-fractured surface of PA-2 blend tested under 3 m/sec: (a) low magnification, (b) and (c) higher magnifications. The inset in (a) describes the SEM observation on fracture surface (shaded)

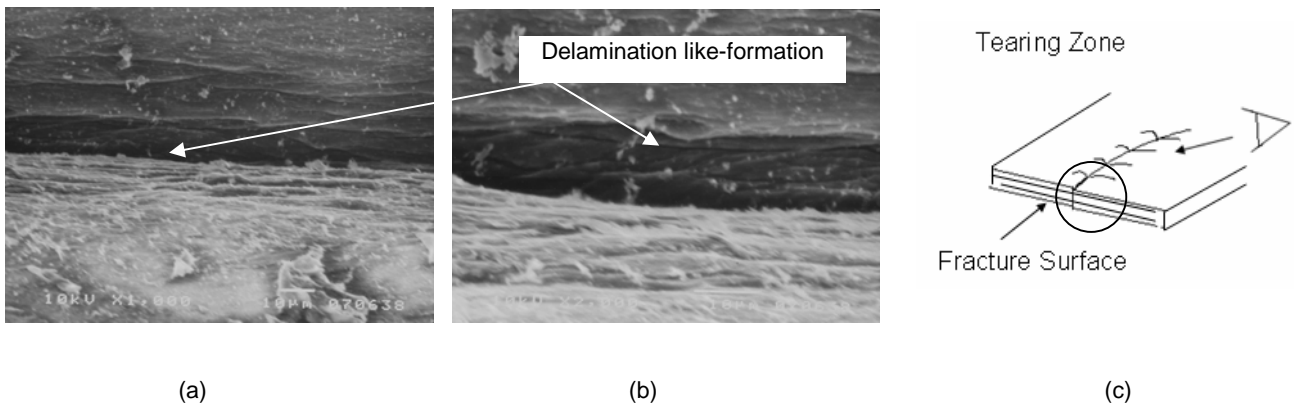


Figure 12. SEM micrographs: (a) and (b) Delamination like-formation found on the tearing zone of PA-1 blend while (c) The view of the observation on tearing zone beneath the fracture surface (shaded)

Shortly, rubber particle size distributed in ABS system has a significant effect on the impact deformation and failure behaviors of the PC/ABS (50/50) blends. It has been pointed out from this work that distribution of smaller bimodal particle in ABS leads to higher crack propagation of the blends. A small particle has smaller diameter and it will induce a smaller region of elevated stress in the surrounding materials than larger particle. When interparticle distance (surface to surface distance) is the same, larger particles will thus interact more than smaller particle. Premature fractures found in the monomodal type of the blends with larger particle size might be caused by too low degree of cross linking that promotes early cavitation in the rubber as deduced in the reference [2].

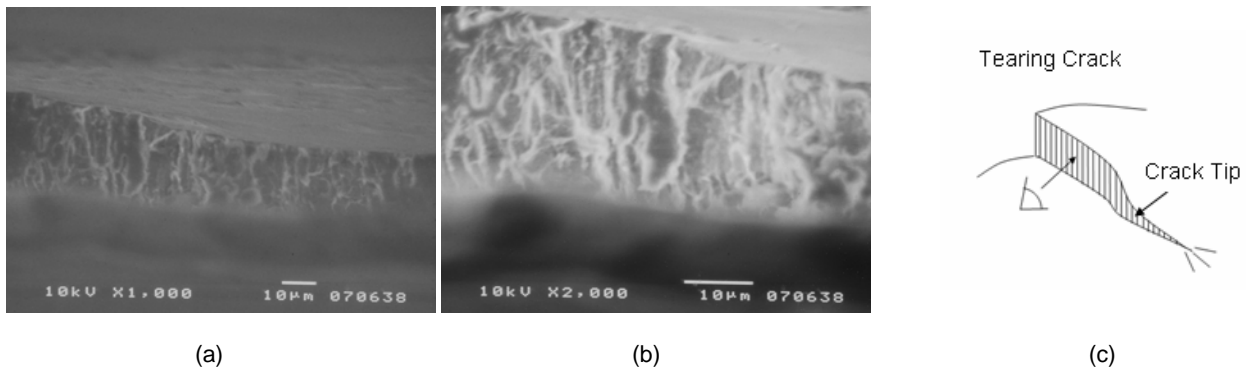


Figure 13. SEM micrographs: (a) and (b) Fibril-like formation zone observed on tearing crack zone of PA-2 while (c) The view of the observation on crack propagation zone (shaded)

Conclusions

The drop weight impact tests have been performed to study the influence of ABS type on the failure characteristics of the two grades of PC/ABS (50/50) blends. In general, these tests revealed that the two grades of the blends fractured in brittle modes when the rate of loading exceeded 3 m/sec. Both monomodal and bimodal types of the blends exhibited similar behavior under 2 and 4 m/sec. At 3 m/sec, their failure modes were significantly different where stress whitening was typical deformation mechanism of the bimodal type of the blends. The PA-1 blend showed the highest impact strength. Basically, impact energy of the bimodal type of the blends as well as ABS materials increased with increasing the loading rates and their impact energy tended to decrease under a certain loading rate at which failure occurred. In other hand, monomodal type of PC/ABS blend tended to decrease with increasing the loading rate and their values were quite lower compare to that of bimodal type of the blends and monomodal type of ABS under higher loading rates. This investigation reveals that blending PC with brittle ABS creates tough PC/ABS blends. Variation of smaller rubber particle distributed in ABS affected reducing in the impact energy of the ABS but blending it into the polycarbonate enhanced the impact energy of PC/ABS (50/50) blends.

The SEM observations on the damage region and fracture surface of each blend correlate well the testing results pointed out that bimodal type of the blends exhibited higher resistance to crack propagation rather than monomodal type. The SEM studies motivate to find the correlation between the quality of polycarbonate and ABS interface and the size of rubber particle embedded in ABS system.

References

1. Wang, T. J., Kishimoto, K., Notomi, M., Ishikawa, M. and Shibuya, T., "Damage and Fracture Behavior of PC/ABS Polymers in Triaxial Stress Fields," First Asian-Australasian Conference on Composite Materials (ACCM-1), Osaka, Japan, October 1998
2. Inberg, J. P. F., "Fracture of Polycarbonate/ABS Blends," University of Twente, Thesis, July 2001.
3. Wildes, G., Keskkula, H. and Paul, D.R., "Fracture Characterization of PC/ABS Blends: Effect of Reactive Compatibilization, ABS Type and Rubber Concentration," *Polymer*, **40**, 7089-7107 (1999)
4. Inberg, J. P. F. and Gaymans, R.J., "Co-continuous Polycarbonate/ABS Blends," *Polymer*, **43 (8)**, 2425-2434 (2002).
5. Inberg, J.P. F., Takens, A. and Gaymans, R.J., "Strain Rate Effects in Polycarbonate and Polycarbonate/ABS Blends," *Polymer*, **43 (9)**, 2795-2802 (2002).
6. Inberg, J.P.F. and Gaymans, R.J., "Polycarbonate and Co-continuous PC/ABS Blends: Influence of Specimen Thickness," *Polymer*, **43 (13)**, 3767-3777(2002).
7. Perkins, W. G., "Polymer Toughness and Impact Resistance, *Polym. Eng. Sci.*, **39 (12)**, 2445-2460 (1999).
8. Kistler, L.S. and Waas, A.M., "Experiment and Analysis on the Response of Curved Laminated Composite Panels Subjected to Low Velocity Impact," *Int. J. Impact Engng.*, **21 (9)**, 711-736 (1998).